International Journal of Thermophysics, Vol. 5, No. 2, 1984

A Dynamic Technique for Measurements of Thermophysical Properties at High Temperatures[1]

A. Cezairliyan[2]

Received February 14, 1984

A technique is described for the dynamic measurement of selected thermophysical properties of electrically conducting solids in the range 1500 K to the melting temperature of the specimen. The technique is based on rapid resistive self-heating of the specimen from room temperature to any desired high temperature in less than 1 s by the passage of an electrical current pulse through it and on measuring the pertinent quantities, such as current, voltage, and temperature, with millisecond resolution. The technique was applied to the measurement of heat capacity, electrical resistivity, hemispherical total emissivity, normal spectral emissivity, thermal expansion, temperature and energy of solid–solid phase transformations, melting temperature, and heat of fusion. Two possible options for the extension of the technique to measurements above the melting temperature of the specimen are briefly discussed. These options are: (1) submillisecond heating of the specimen and performance of the measurements with microsecond resolution, and (2) performance of the experiments in a near-zero-gravity environment with millisecond resolution.

KEY WORDS: electrical resistivity; heat capacity; heat of fusion; hemispherical total emissivity; high-speed techniques; high temperatures; melting temperature; normal spectral emissivity; phase transformation; thermal expansion.

1. INTRODUCTION

Conventional steady-state and quasi-steady-state techniques for accurate measurement of thermophysical properties are generally limited to tempera-

[1] Paper presented at the Japan–United States Joint Seminar on Thermophysical Properties, October 24–26, 1983, Tokyo, Japan.

[2] Thermophysics Division, National Bureau of Standards, Washington, D.C. 20234, U.S.A.

0195-928X/84/0600-0177$03.50/0

tures below 2000 K. This limitation is the result of severe problems (chemical reactions, heat transfer, evaporation, specimen containment, loss of mechanical strength and electrical insulation, etc.) created by the exposure of the specimen and its immediate environment to high temperatures for extended periods of time (minutes to hours). An approach to minimize the effect of these problems and thus to permit the extension of the measurements to higher temperatures is to perform the entire experiment in a very short period of time (less than 1 s). It is in this context that most of the dynamic techniques for the measurement of thermophysical properties at high temperatures were developed.

The development of various dynamic techniques for the measurement of selected thermophysical properties of electrically conducting substances have been reviewed in the literature [1–4]. The objective of this paper is to describe briefly the technique developed at the National Bureau of Standards, summarize the investigations performed with the technique during the past decade, and present some of the recent advances. The technique was applied to the measurement of heat capacity, electrical resistivity, hemispherical total emissivity, normal spectral emissivity, thermal expansion, temperature and energy of solid–solid phase transformations, melting temperature, and heat of fusion.

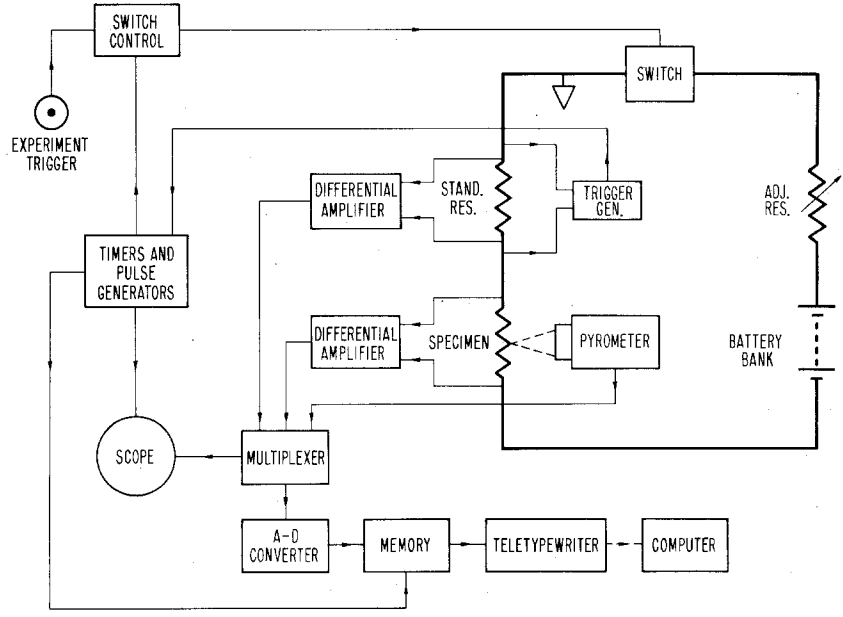

Fig. 1. Functional diagram of the dynamic thermophysical measurement system [6].

2. METHOD AND MEASUREMENT SYSTEM

The method is based on resistive self-heating of the specimen from room temperature to any high temperature (in the range from 1500 K to its melting temperature) in less than 1 s by the passage of an electrical current pulse through it; and on measuring, with millisecond resolution, such experimental quantities as current through the specimen, voltage across the specimen, and specimen temperature. Formulation of the relations for properties in terms of the experimental quantities are given in an earlier publication [5].

The measurement system consists of an electric power pulsing circuit and associated measuring and control circuits. A functional diagram of the complete system is presented in Fig. 1. The details of the measurement system and its operational characteristics are given in earlier publications [5, 6]. In this section, some of the important features are summarized.

2.1. Pulse Circuit

The pulse circuit includes the specimen in series with a battery bank, a standard resistance, an adjustable resistance, and a switching system. The battery bank consists of 14 series-connected 2-V batteries each having approximately 1100 A · h capacity. A standard resistance (1 mΩ) is used to measure the pulse current through the specimen. An adjustable resistance (total resistance 30 mΩ) enables control of the heating rate of the specimen and the shape of the current pulse. The switching system consists of two series-connected, fast-acting switches. The second switch is used as a backup in the event the first one fails to open at the end of the heating period.

2.2. Specimen and Experiment Chamber

The specimen is a tube of the following nominal dimensions: length, 75–100 mm; outside diameter 6 mm; and wall thickness, 0.5 mm. A small rectangular hole (1 × 0.5 mm) is fabricated in the wall at the middle of the specimen to approximate blackbody conditions for pyrometric temperature measurements. For the above geometry, blackbody quality of the sighting hole is estimated to be approximately 0.99. Depending on the investigation, specimens of other geometrical forms (rods, strips) may be used. The specimen is mounted vertically 6 mm off-center with respect to the axis of the experiment chamber to reduce the effect of internal reflections. The chamber wall and the specimen clamps are water-cooled. Thermocouples are connected (electrically insulated) to the two end clamps to measure the

specimen temperature before each pulse experiment. An expansion joint allows the expansion of the specimen in the downward direction. The voltage probes are knife edges made of the specimen material and are placed at a distance approximately 13 mm from the end clamps. The knife edges define a portion of the specimen, which should be free of axial temperature gradients for the duration of the experiment. The chamber is designed for conducting experiments with the specimen either in vacuum or in a controlled atmosphere. A schematic diagram of the experiment chamber is shown in Fig. 2.

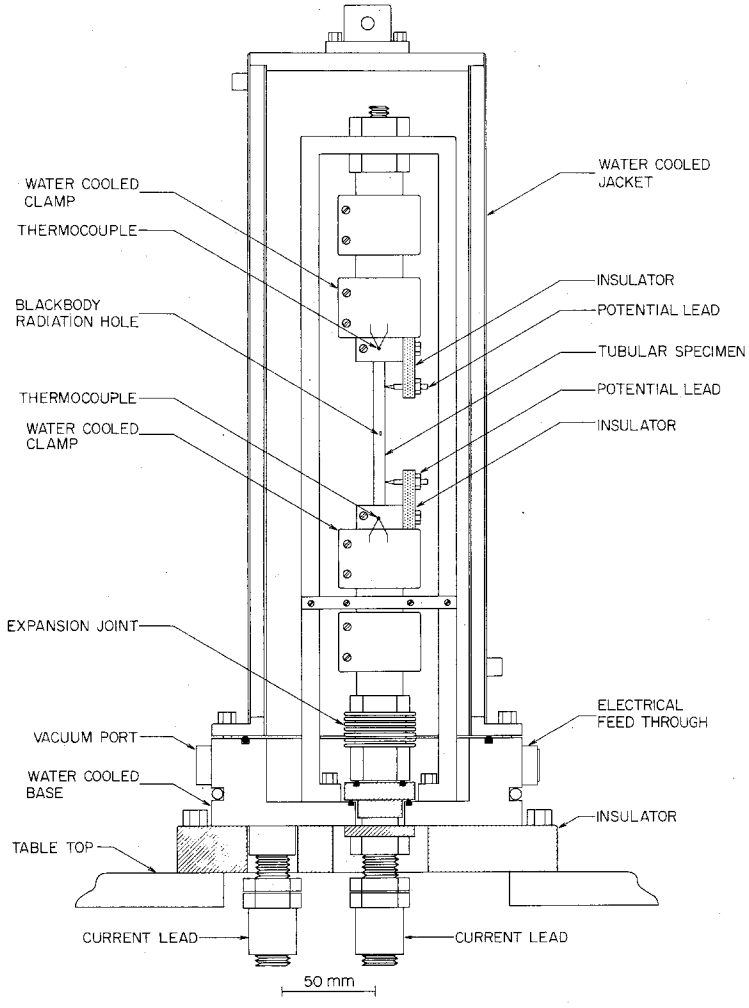

Fig. 2. Schematic diagram of the experiment chamber [6].

2.3. High-Speed Pyrometer

Temperature of the specimen is measured with a high-speed photoelectric pyrometer, which permits 1200 evaluations of the specimen temperature per second. The pyrometer alternatively passes precisely timed samples of radiance from the specimen and a reference source (gas-filled tungsten filament lamp) through an interference filter (wavelength 653 nm, bandwidth 10 nm) to a photomultiplier. During each exposure, the photomultiplier output is integrated and is recorded. For measurements at temperatures above 2500 K, calibrated optical attenuators are placed in the path of the radiation from the specimen. The pyrometer target is a circular area 0.2 mm in diameter. The details regarding the construction and operation of the pyrometer are given in the literature [7].

2.4. Data Recording System

Data corresponding to temperature, current, and voltage are recorded with a high-speed digital data acquisition system, which consists of a multiplexer, analog-to-digital converter, and a core memory together with control and interfacing equipment. All signals are brought to the multiplexer through differential amplifiers in order to avoid inaccuracies arising from common ground points. The multiplexed signals go to the analog-to-digital converter, which has a full-scale reading of ± 10 V and a full-scale resolution of one part in 8192 ($8192 = 2^{13}$). Digital output from the converter consists of 13 binary bits plus a sign bit. This output is stored in a core memory having a capacity of 2048 words of 16 bits each. The data acquisition system is capable of recording a set of signals corresponding to temperature, voltage, and current approximately every 0.4 ms. At the end of the pulse experiment, data stored in the memory are transferred to a minicomputer for processing. An oscilloscope is used only to monitor the general pattern of the experimental results, and to detect any anomalies.

2.5. Typical Operational Characteristics

The operational characteristics of the system depend primarily on the electrical circuit parameters, properties of the specimen, and specimen maximum temperature. The system characteristics for typical experiments are as follows: current, 1–3 kA; power, 5–15 kW; heating rate, 3–9 $K \cdot ms^{-1}$; heating duration 0.3–0.9 s; heating rate/cooling rate, 10–100. The above figures are the results of typical experiments and do not represent the full capabilities of the measurement system.

3. MEASUREMENT OF PROPERTIES

In the following paragraphs, the capabilities of the system from the viewpoint of measured properties are briefly discussed. Whenever pertinent,

Table I. Summary of Investigations with the Dynamic Thermophysical Measurement System

Investigator[a]	Year	Ref.	Substance	Property[b]	Temperature range (K)
CeMoBerBec	1970	5	Mo	$c, \rho, \epsilon, \epsilon_\lambda$	1900–2800
CeMoBec	1970	8	Mo	T_m, ρ	2840–2894
Ce	1971	9	Nb	$c, \rho, \epsilon, \epsilon_\lambda$	1500–2700
CeMc	1971	10	W	$c, \rho, \epsilon, \epsilon_\lambda$	2000–3600
CeMcBec	1971	11	Ta	$c, \rho, \epsilon, \epsilon_\lambda$	1900–3200
Ce	1972	12	Nb	$T_m, \rho, \epsilon_\lambda$	2650–2750
Ce	1972	13	Ta–10W	c, ρ, ϵ	1500–3200
Ce	1972	14	W	T_m, ρ	3600–3695
Ce	1973	15	Nb–1Zr	c, ρ, ϵ	1500–2700
Ce	1973	16	Nb	T_r	2750
Ce	1974	17	Nb–10Ta–10W	c, ρ, ϵ	1500–2800
CeMc	1974	18	Fe	c, ρ, ϵ, T_m	1500–1808
CeRi	1974	19	Zr	c, ρ, ϵ	1500–2100
CeRiMc	1974	20	V	c, ρ, ϵ	1500–2100
CeMc	1975	21	Hf–3Zr	c, ρ, ϵ	1500–2400
CeMc	1975	22	Fe	T_r	1808
CeMc	1975	23	Fe	$T_t, Q_t, \epsilon_\lambda$	1683
CeRi	1975	24	C	c, ρ, ϵ	1500–3000
CeRi	1975	25	Zr	T_m, T_r, ρ	2100–2128
CeRi	1975	26	Zr	T_t, Q_t	1147
CeCoRiRo	1975	27	Mo	T_r	2894
CeMc	1976	28	Hf–3Zr	T_m, T_r	2471

CeMc	1976	29	Hf–3Zr	T_t, Q_t, ϵ_λ	2012
CeMcCoRiRo	1976	30	Ta	T_r	3270
CeMi	1977	31	Ti	c, ρ, ϵ	1500–1900
CeMi	1977	32	Ti	T_m, ρ, ϵ_λ	1900–1945
CeMcT	1977	33	Ti–6Al–4V	c, ρ, ϵ, T_m	1450–1943
RiRoCoCeMc	1977	34	Ti	T_r	1945
CeMi	1978	35	Ti	T_t, Q_t	1166
MiCe	1979	36	Pd	T_r	1827
CeMiRiRo	1979	37	V	T_r	2193
CeMi	1980	38	SS304	c, ρ, ϵ, T_m	1400–1707
MiCe	1980	39	Pd	c, ρ	1400–1800
CeMi	1980	40	Nb	Q_m	2750
CeMi	1980	41	C-comp.	c, ρ	1500–3000
Ce	1980	42	Mo	ρ	1500–2650
MiCe	1981	43	Pd	T_m	1827
CeMi	1982	44	W	T_r	3208
MiCe	1982	45	Ta	α	1500–3200
Ce	1983	46	Mo	c	1500–2800
CeMi	1983	47	Ni	c, ρ	1300–1700
CeMi	1984	48	Ni	T_m	1729
MiCe	1984	49	Fe	α	1130–1330
CeMi	1984	50	W–3Re	c, ρ, ϵ, T_m	1500–3645

[a] Bec, Beckett; Ber, Berman; Co, Coslovi; Ce, Cezairliyan; Mc, McClure; Mi, Miiller; Ri, Righini; Ro, Rosso; T, Taylor.

[b] The property symbol designations are as follows: c, heat capacity at constant pressure; Q_t, energy of solid–solid phase transformation; Q_m, heat of fusion; T_m, melting temperature; T_r, radiance temperature at melting temperature; T_t, temperature of solid–solid phase transformation; α, thermal expansion; ϵ, hemispherical total emissivity; ϵ_λ, normal spectral emissivity at 653 nm; ρ, electrical resistivity.

key references to more detailed presentations are given. A summary of the measurements of properties of substances that have been performed with the system is given in Table I.

3.1. Heat Capacity

Heat capacity is determined from the measurements of voltage, current, and temperature during the heating period. A correction for heat loss from the specimen due to thermal radiation is made based on hemispherical total emissivity determined during the same experiment. The measurement and computational details regarding heat capacity are given in the literature [5].

3.2. Electrical Resistivity

Electrical resistivity is obtained from the measurement of voltage, current, and temperature during the heating period. The measurement and computational details regarding electrical resistivity are given in the literature [5].

3.3. Hemispherical Total Emissivity

Hemispherical total emissivity is obtained from data taken during the heating period in conjunction with temperature measured during the initial cooling period that follows the heating period. The measurement and computational details regarding hemispherical total emissivity are given in the literature [5].

3.4. Normal Spectral Emissivity

Normal spectral emissivity is measured at the effective wavelength of the pyrometer's interference filter (wavelength 653 nm, bandwidth 10 nm). For this determination, two rapid heating experiments are performed in which the pyrometer is aimed first at the blackbody radiation hole and then at the surface of the tubular specimen. The ratio of radiance (surface to hole) corresponding to the same specimen temperature is the normal spectral emissivity. The same temperature in the two experiments is found by matching the measured specimen resistance. The measurement and computational details regarding normal spectral emissivity are given in the literature [5].

3.5. Thermal Expansion

Recently, it was demonstrated that the system, with some additions, can be used to measure the thermal expansion of metals. The technique is based on simultaneously measuring, during rapid heating of the specimen,

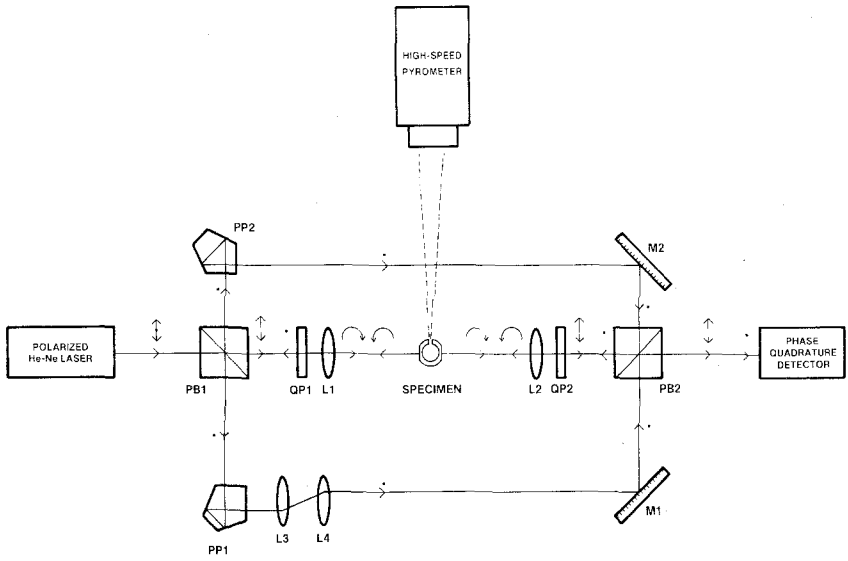

Fig. 3. Schematic diagram of the interferometer consisting of the following optical elements: polarizing beamsplitters PB1 and PB2; quarter-wave plates QP1 and QP2; lenses L1, L2, L3, and L4; pentaprisms PP1 and PP2; and plane mirrors M1 and M2. The double-headed arrows, the heavy dots, and the curved arrows refer to the polarization states of the component beams. The specimen is shown in cross section [45].

the specimen expansion by the shift in the fringe pattern produced by a Michelson-type polarized beam interferometer and the specimen temperature by means of the high-speed pyrometer. The specimen, fabricated into the form of a precision-machined tube with parallel optical flats on opposite sides along the length, is placed as a double reflector in the path of one of the two light beams. The schematic representation of the interferometer for rapid thermal expansion measurements is shown in Fig. 3. The measurements and the computational details regarding thermal expansion are given in the literature [45].

3.6. Temperature and Energy of Solid–Solid Phase Transformation

For studies related to the temperature and energy of the solid–solid transformations that take place quickly (in less than 1 ms) the present dynamic technique can be applied. Most significant first-order solid–solid phase transformations in a specimen are manifested by a plateau in the temperature versus time function during its heating or cooling. The average of the measured temperatures at the plateau yields the transformation temperature. From the integral of the power absorbed by the specimen

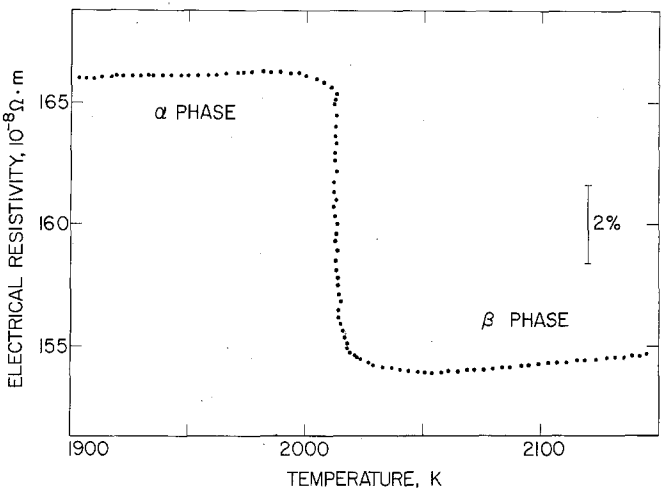

Fig. 4. Variation of the electrical resistivity as a function of temperature of a hafnium specimen near and at its solid–solid transformation temperature [29].

during the transformation, the transformation energy is obtained. In addition, from the measurements of voltage and current, the variation in the electrical resistivity of the specimen during the transformation can be obtained (Fig. 4). The measurement and computational details regarding temperature and energy of solid–solid transformation are given in the literature [29].

3.7. Melting Temperature

During rapid heating of the tubular specimen, if the current is not interrupted the specimen temperature reaches its melting temperature, and then the specimen collapses under gravitational force. Melting is manifested by a plateau in the temperature versus time function. By averaging the temperature points on the plateau, the melting temperature is obtained. The results of a typical experiment on the melting of niobium is shown in Fig. 5. The measurement and computational details regarding the melting temperature are given in the literature [8].

3.8. Radiance Temperature at the Melting Temperature

If strip-shaped specimens are used for the melting temperature experiments instead of the tubular specimens, one obtains the radiance temperature as the specimen melts. During the initial melting period, the radiance temperature of strip specimens yields a horizontal plateau. The results of two typical experiments on tungsten are given in Fig. 6. The drop in

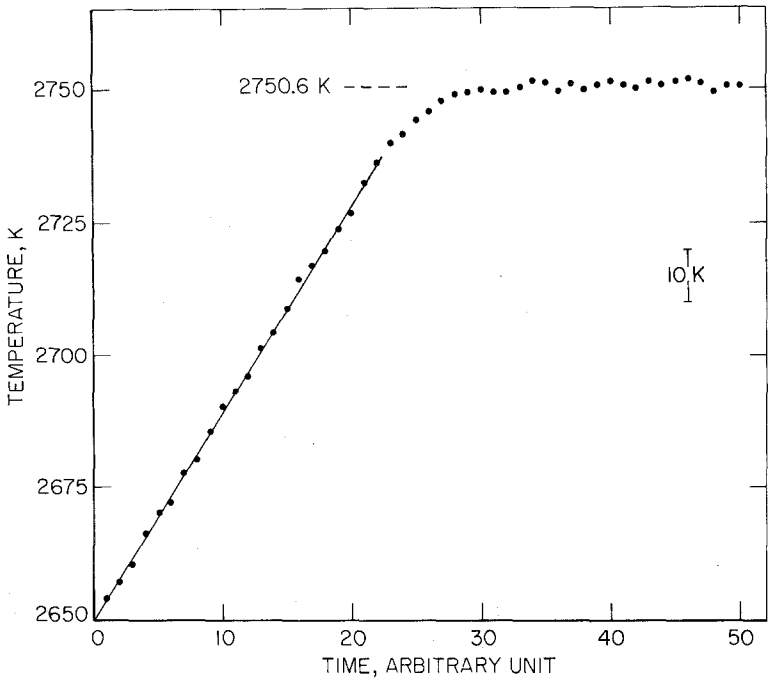

Fig. 5. Variation of the temperature of a niobium specimen near and at its melting temperature [12].

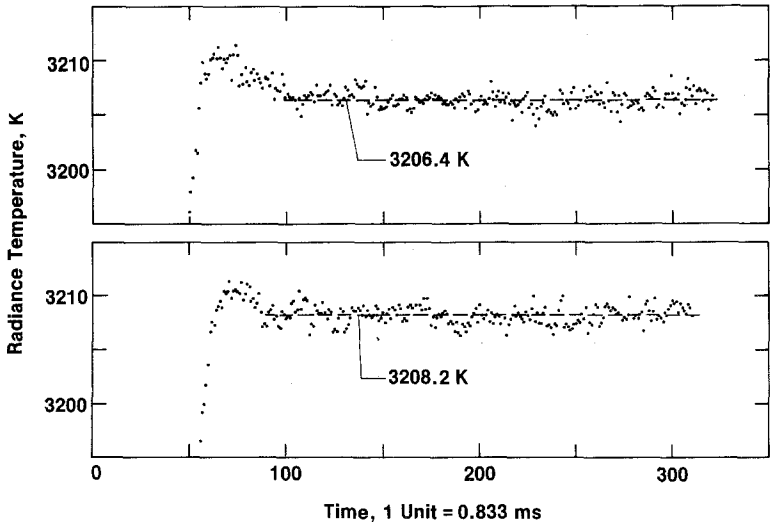

Fig. 6. Variation of radiance temperature (at 653 nm) as a function of time near and at the melting temperature of tungsten for two typical experiments [44].

temperature just as the plateau starts corresponds to a change (decrease) in the normal spectral emissivity of the specimen as it starts to melt. This is likely to be the case, in general, since solid surfaces, regardless of the degree of polish, depart from the conditions of ideal smoothness. The averages of the temperatures at the plateau for different specimens of the same metal were found to be reproducible, usually within a few degrees kelvin. The measurement and computational details regarding radiance temperature at the melting temperature are given in the literature [16]. Because of the simplicity and ease of performing experiments with strips, radiance temperature measurements at the melting temperature of selected metals may find applications in performing secondary calibrations on instruments and in conducting overall *in situ* checks on complicated measurement systems at high temperatures. The combination of the measurement of the true melting temperature and the radiance temperature at the melting temperature yields the normal spectral emissivity of the specimen at its melting temperature.

3.9. Heat of Fusion

The feasibility of measuring heat of fusion was demonstrated in experiments where a composite specimen consisting of three strips (each 76 mm long, 6.3 mm wide, 0.25 mm thick) in parallel was used (Fig. 7). The

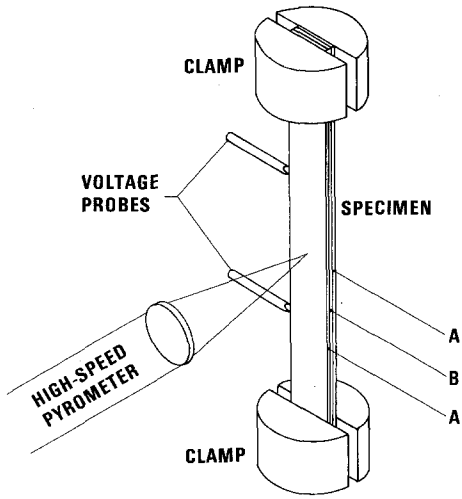

Fig. 7. Schematic diagram showing the arrangement of the composite specimen, clamps, and radiance temperature measurement system (dimension not to scale). Strip of material B is sandwiched between two strips of material A. The melting temperature of B is lower than that of A [40].

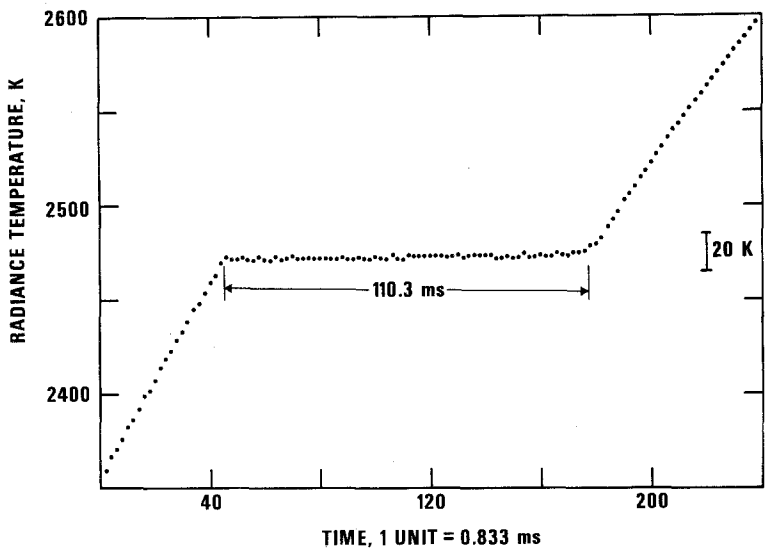

Fig. 8. Variation of radiance temperature of a composite specimen as a function of time during its heating period. The inner strip is niobium, and the outer strips are tantalum. The plateau corresponds to the melting of niobium [40].

two outer strips were made of tantalum and the inner strip was made of niobium. Other combinations may also be used as long as the melting temperature of the inner strip is lower than that of the outer strips. The function of the outer strips is to contain the inner metal during the melting period. The result of a typical experiment that shows the radiance temperature of the outer strip of a composite specimen near and at the melting temperature of niobium is presented in Fig. 8. Heat of fusion was obtained by integrating the power absorbed by the niobium strip over the duration of the plateau. Heat loss due to thermal radiation was taken into consideration. The measurement and computational details regarding heat of fusion are given in the literature [40].

3.10. Estimate of Errors

A summary of the imprecision and estimated uncertainty of measured quantities and properties with the dynamic thermophysical measurement system is given in Table II. The values represent typical results for measurements in the range 2000–2500 K. Imprecision and uncertainty of most quantities in dynamic measurements are somewhat insensitive to temperature and do not increase significantly with temperature. The details regarding the estimates of errors and their combination for most of the properties

Table II. Typical Values of Imprecision and Estimated Uncertainty of Measured Quantities and Properties with the Dynamic Thermophysical Measurement System[a]

Quantity	Imprecision	Uncertainty
Temperature	0.5 K	5 K
Voltage	0.03%	0.1%
Current	0.03%	0.1%
Heat capacity	0.5%	2–3%
Electrical resistivity	0.1%	0.5–1%
Hemispherical total emissivity	1%	3–5%
Normal spectral emissivity (at 0.65 μm)	1%	3–5%
Thermal expansion	0.5%	1–2%
Transformation (solid–solid) temperature	1 K	5–10 K
Transformation (solid–solid) energy	2 %	5–10%
Melting temperature	1 K	5–10 K
Heat of fusion	2%	5–10%

[a] Imprecision refers to the standard deviation of an individual point as computed from the difference between the measured value and that from the smooth function obtained by the least-squares method. Uncertainty refers to the estimated total error (random and systematic). Values correspond to measurements in the range 2000–2500 K.

listed in the table were given in an earlier publication [5]. For properties that have been added more recently, the reader may consult the pertinent individual papers referenced above.

4. EXTENSION OF MEASUREMENTS TO PROPERTIES OF LIQUIDS

The dynamic technique described in this paper is for the measurement of properties of solid electrical conductors above about 1500 K. The upper temperature of the measurements has been limited by the melting temperature of the specimen, at which point the specimen becomes unstable and collapses. Two possible options for the extension of the measurements to temperatures above the melting temperature are: (1) submillisecond heating of the specimen, which requires performance of the pertinent measurements with microsecond resolution, and (2) performance of the experiments in a near-zero-gravity environment with millisecond resolution.

1. The principle of the microsecond-resolution dynamic measurement technique is the same as that described earlier for the millisecond-resolution technique. The major difference is in the power supply; a capacitor bank is utilized for the microsecond-resolution system to enable heating of the specimen in times shorter than 1 ms. Also, because of the increased speed, measurement of the experimental quantities becomes much more difficult and as a result less accurate than in the millisecond-resolution case. Up to

now, research in this area has been mostly of an exploratory nature; however, the results have indicated the feasibility of measuring the enthalpy, electrical resistivity, and thermal expansion of liquid metals up to about 10,000 K. A summary of such investigations reported in the literature is given in Ref. 4. An accurate microsecond-resolution system under development at the National Bureau of Standards is described in the literature [51].

2. If the experiments are performed in a near-zero-gravity environment, it may be possible for the specimen to sustain its geometry (cylindrical liquid column) above the melting temperature for the duration of the dynamic experiment. This technique is likely to extend the measurements to several hundred and possibly several thousand degrees above the melting temperature. Research is presently under way at the National Bureau of Standards to assess the feasibility of this method. The problems that are being studied include: (1) the effect of forces other than the gravitational force, such as surface tension, and electromagnetic forces, on the stability of the specimen in the form of a liquid column, (2) the optimum geometry for the specimen from stability viewpoint, and (3) the effect of perturbations due to vibration, expansion, etc.

5. DISCUSSION

The dynamic technique described in this paper has been used successfully for the measurement of several thermophysical and related properties in the range from 1500 K to the melting temperature of the specimen. The technique has been perfected to a level of competitiveness with the most accurate conventional steady-state techniques in the overlapping temperature range (1500–2000 K) for the two types of techniques.

At temperatures above 2000 K, it becomes very difficult if not impossible to perform accurate steady-state experiments; thus the dynamic technique becomes a unique and indispensable tool for thermophysical measurements at high temperatures. The dynamic technique has the added advantage of covering a wide temperature range in a single experiment and of yielding high resolution in temperature measurements in comparison with most of the conventional techniques. This is an important feature, especially in measurements near and at phase transformations.

The potential of the dynamic technique has not been explored completely. In addition to the properties investigated so far, the dynamic technique may be used to measure other thermal, electrical, and related properties in both the solid and liquid phases, as well as to measure properties of more complex substances, such as certain carbides, borides, nitrides, and oxides. An added advantage of the dynamic technique is that

it may provide the means of studying time-dependent phenomena in substances.

ACKNOWLEDGMENT

The work described in this paper was supported in part by the U. S. Air Force Office of Scientific Research.

REFERENCES

1. A. Cezairliyan, *High Temp.-High Press.* **1**:517 (1969).
2. A. Cezairliyan, *Rev. Int. Hautes Temp. Réfract.* 7:215 (1970).
3. A. Cezairliyan and C. W. Beckett, Electrical discharge techniques for measurements of thermodynamic properties of fluids at high temperatures, in *Experimental Thermodynamics of Non-Reacting Fluids*, B. Le Neindre and B. Vodar, eds. (Butterworths, London, 1975), p. 1161.
4. A. Cezairliyan, *High Temp.-High Press.* **11**:9 (1979).
5. A. Cezairliyan, M. S. Morse, H. A. Berman, and C. W. Beckett, *J. Res. Nat. Bur. Stand.* **74A**:65 (1970).
6. A. Cezairliyan, *J. Res. Nat. Bur. Stand.* **75C**:7 (1971).
7. G. M. Foley, *Rev. Sci. Instrum.* **41**:827 (1970).
8. A. Cezairliyan, M. S. Morse, and C. W. Beckett, *Rev. Int. Hautes Temp. Réfract.* 7:382 (1970).
9. A. Cezairliyan, *J. Res. Nat. Bur. Stand.* **75A**:565 (1971).
10. A. Cezairliyan and J. L. McClure, *J. Res. Nat. Bur. Stand.* **75A**:283 (1971).
11. A. Cezairliyan, J. L. McClure, and C. W. Beckett, *J. Res. Nat. Bur. Stand.* **75A**:1 (1971).
12. A. Cezairliyan, *High Temp.-High Press.* **4**:453 (1972).
13. A. Cezairliyan, *High Temp.-High Press.* **4**:541 (1972).
14. A. Cezairliyan, *High Temp. Sci.* **4**:248 (1972).
15. A. Cezairliyan, *J. Res. Nat. Bur. Stand.* **77A**:45 (1973).
16. A. Cezairliyan, *J. Res. Nat. Bur. Stand.* **77A**:333 (1973).
17. A. Cezairliyan, *J. Chem. Thermodynamics* **6**:735 (1974).
18. A. Cezairliyan and J. L. McClure, *J. Res. Nat. Bur. Stand.* **78A**:1 (1974).
19. A. Cezairliyan and F. Righini, *J. Res. Nat. Bur. Stand.* **78A**:509 (1974).
20. A. Cezairliyan, F. Righini, and J. L. McClure, *J. Res. Nat. Bur. Stand.* **78A**:143 (1974).
21. A. Cezairliyan and J. L. McClure, *J. Res. Nat. Bur. Stand.* **79A**:431 (1975).
22. A. Cezairliyan and J. L. McClure, *J. Res. Nat. Bur. Stand.* **79A**:541 (1975).
23. A. Cezairliyan and J. L. McClure, *High Temp. Sci.* 7:189 (1975).
24. A. Cezairliyan and F. Righini, *Rev. Int. Hautes. Temp. Réfract.* **12**:124 (1975).
25. A. Cezairliyan and F. Righini, *Rev. Int. Hautes. Temp. Réfract.* **12**:201 (1975).
26. A. Cezairliyan and F. Righini, *J. Res. Nat. Bur. Stand.* **79A**:81 (1975).
27. A. Cezairliyan, L. Coslovi, F. Righini, and A. Rosso, Radiance temperature of molybdenum at its melting point, in *Temperature Measurement—1975*, B. F. Billing and T. J. Quinn, eds. (Conference Series No. 26, Institute of Physics, London, 1975), p. 287.
28. A. Cezairliyan and J. L. McClure, *J. Res. Nat. Bur. Stand.* **80A**:659 (1976).
29. A. Cezairliyan and J. L. McClure, *High Temp.-High Press.* **8**:461 (1976).
30. A. Cezairliyan, J. L. McClure, L. Coslovi, F. Righini, and A. Rosso, *High Temp.-High Press.* **8**:103 (1976).
31. A. Cezairliyan and A. P. Miiller, *High Temp.-High Press.* **9**:319 (1977).
32. A. Cezairliyan and A. P. Miiller, *J. Res. Nat. Bur. Stand.* **82**:119 (1977).
33. A. Cezairliyan, J. L. McClure, and R. Taylor, *J. Res. Nat. Bur. Stand.* **81A**:251 (1977).
34. F. Righini, A. Rosso, L. Coslovi, A. Cezairliyan, and J. L. McClure, Radiance temperature of titanium at its melting point, in *Proceedings of the Seventh Symposium on*

Thermophysical Properties, A. Cezairliyan, ed. (American Society of Mechanical Engineers, New York, 1977), p. 312.
35. A. Cezairliyan and A. P. Miiller, *J. Res. Nat. Bur. Stand.* **83**:127 (1978).
36. A. P. Miiller and A. Cezairliyan, *High Temp. Sci.* **11**:41 (1979).
37. A. Cezairliyan, A. P. Miiller, F. Righini, and A. Rosso, *High Temp. Sci.* **11**:223 (1979).
38. A. Cezairliyan and A. P. Miiller, *Int. J. Thermophys.* **1**:83 (1980).
39. A. P. Miiller and A. Cezairliyan, *Int. J. Thermophys.* **1**:217 (1980).
40. A. P. Miiller and A. Cezairliyan, *Int. J. Thermophys.* **1**:195 (1980).
41. A. Cezairliyan and A. P. Miiller, *Int. J. Thermophys.* **1**:317 (1980).
42. A. Cezairliyan, *Int. J. Thermophys.* **1**:417 (1980).
43. A. P. Miiller and A. Cezairliyan, *Int. J. Thermophys.* **2**:63 (1981).
44. A. Cezairliyan and A. P. Miiller, *Int. J. Thermophys.* **3**:89 (1982).
45. A. P. Miiller and A. Cezairliyan, *Int. J. Thermophys.* **3**:259 (1982).
46. A. Cezairliyan, *Int. J. Thermophys.* **4**:159 (1983).
47. A. Cezairliyan and A. P. Miiller, *Int. J. Thermophys.* **4**:389 (1983).
48. A. Cezairliyan and A. P. Miiller, *Int. J. Thermophys.* **5**:315 (1984).
49. A. P. Miiller and A. Cezairliyan, Thermal expansion of iron during the $\alpha \rightarrow \gamma$ phase transformation by a transient interferrometric technique, in *Thermal Expansion—8*, T. A. Hahn, ed. (Plenum Press, New York, in press).
50. A. Cezairliyan and A. P. Miiller, *Int. J. Thermophys.* (in press).
51. A. Cezairliyan, M. S. Morse, G. M. Foley, and N. E. Erickson, Microsecond resolution pulse heating technique for thermophysical measurements at high temperatures, in *Proceedings of the Eighth Symposium on Thermophysical Properties*, Vol. II, J. V. Sengers, ed. (American Society of Mechanical Engineers, New York, 1982), p. 45.